ELSEVIER

Journal of Materials Processing Technology 114 (2001) 75–86

Journal of Materials Processing Technology

www.elsevier.com/locate/jmatprotec

Computer aided rheological design of extrusion dies for profiles

O.S. Carneiro[a,*], J.M. Nóbrega[a], F.T. Pinho[b], P.J. Oliveira[c]

[a]*Department of Polymer Engineering, Universidade do Minho, Campus de Azurém, 4800-058 Guimarães, Portugal*
[b]*Centro de Estudos de Fenómenos de Transporte, DEMEGI, Faculdade de Engenharia da Universidade do Porto, Rua Roberto Frias, 4200-465 Porto, Portugal*
[c]*Departamento de Engenharia Electromecânica, Universidade da Beira Interior, Rua Marquês D'Ávila e Bolama, 6200 Covilhã, Portugal*

Received 20 February 2001; received in revised form 20 February 2001; accepted 2 March 2001

Abstract

A global methodology for the rheological design of profile extrusion dies is proposed. This methodology accounts for: (i) flow defects due to maximum admissible stresses, pressure drop and melt temperature increase; (ii) post-extrusion phenomena (shrinkage upon cooling, draw-down promoted by pulling and swelling after die exit) and (iii) flow balancing. The part of the methodology, that is concerned with flow balancing, was implemented and is here illustrated in two case studies, each one leading to the adoption of a different constructive solution. The software is based on a finite-volume method, which performs the required three-dimensional simulations, and is also briefly described. © 2001 Elsevier Science B.V. All rights reserved.

Keywords: Extrusion die design; Profiles; Flow balancing; Finite-volume

1. Introduction

The performance of extrusion dies depends, amongst other things, on the rheological design of the flow channel and on the operating conditions adopted during extrusion. An adequate design must guarantee the production of the required profile (in terms of geometry and dimensions) at the highest possible speed and quality. This requires the minimum possible level of internal stresses and the avoidance of rheological defects (e.g., shark skin and melt fracture) and thermal degradation of the melt. To fulfil these objectives the rheological design of these extrusion tools must consider:

1. the maximum flow rate above which there is shark skin at the die exit,
2. the maximum angle of convergence above which melt fracture in extension-dominated flows occurs,
3. the correction of the cross-section of the parallel zone to anticipate post-extrusion effects,
4. the design of the final die zone required to balance the flow at the die exit, i.e., to attain the same average melt velocity in the various parallel zones of the die exit cross-section, in order to minimise the development of internal stresses,
5. the control over both the total pressure drop and the appearance of hot spots (local increases in melt temperature) resulting from internal viscous dissipation.

The viscoelastic behaviour of the polymer melts and the large number of phenomena and restrictions involved makes this a very complex task, which is strongly dependent on the designer knowledge and experience and often requires several trials. Considerable gains are to be expected from the use of adequate computational tools, but despite the availability of some commercial software for the numerical prediction of polymer melt flows through extrusion dies [1–5], its application still requires the user to take decisions in order to generate the successive trial geometries until a final reasonable solution is achieved. Furthermore, the commercial codes usually do not include all the relevant phenomena: for example, it is already possible to solve the inverse problem in die-swell, i.e., to guess the contour of the die land required to produce a given profile [6,7], but without considering the effect of draw-down and the need of flow balancing, which only recently has been addressed in the literature [8–11]. At the same time these computational tools are usually not user-friendly and require large CPU times, which are incompatible with the industrial need of swift calculations. The global automatic optimisation of extrusion die design still remains a challenge [11] and it is the purpose of this work to contribute to further developments of automatic die design tools.

* Corresponding author. Fax: +351-253510249.

0924-0136/01/$ – see front matter
PII: S0924-0136(01)00574-X

In this work, a global methodology for the rheological design of profile extrusion dies is proposed. It not only includes the most relevant phenomena involved but also makes use of some practical know-how in order to guarantee the achievement of a realistic solution. The structure adopted is adequate for its future inclusion in an automatic process of optimisation of the flow channel geometry. A 'first guess' is based on analytical calculations, and is followed by numerical simulations aimed at refining the solution, in order to increase the efficiency of the optimisation process. The numerical calculations of the flow field are based on a finite-volume code for the solution of the mass, momentum and rheological constitutive equations [12]. This code solves the three-dimensional flow of Newtonian, generalised Newtonian or more complex viscoelastic fluids (the user-selected constitutive equation) and it significantly contributes to reduce the time required to perform all the simulations needed to achieve the geometrical solution.

The next section defines the major geometrical components of a die and gives an overview of the global methodology required to undertake its rheological design, which constitutes the main contribution of this work. In Section 3, the numerical code used to perform the simulations is described in more detail. In Section 4, the part of the methodology concerning flow balancing is applied to the design of some profile extrusion dies the results of which are presented and discussed in Section 5. The paper ends with a summary of the main conclusions.

2. Methodology

The design of an extrusion die is an iterative process, made of several main steps: it starts with a tentative definition of the exit shape and dimensions (die lips) and progresses upstream to end at the entrance (discharge zone of the extruder). Each step of this process is associated with a particular geometrical zone, namely the die land or parallel zone (PZ), the pre-parallel zone (PPZ), the transition zone (TZ) and the adapter (A), all shown in Fig. 1.

The parallel, transition and adapter zones are present in almost all conventional dies. Since the flow balancing cannot be attained by modifications performed in the die land cross-section, as that would change the extrudate dimensions, in the present methodology a pre-parallel zone was inserted between the transition and the parallel zones. The pre-parallel zone is convergent and, as the parallel zone, it is very restrictive to the flow. The insertion of that zone facilitates the local control of the flow resistance and will not influence the final extrudate dimensions if a sufficiently long parallel zone is provided. The controllable geometrical parameters of the pre-parallel zone are those shown in Fig. 2: (L) length with constant thickness, (α) angle of convergence and (t_2/t_1) compression ratio.

The design algorithm, depicted schematically in Fig. 3, shows the four main tasks of the proposed methodology. In Task 1, the first trial geometry of the parallel and pre-parallel zones is established using analytical relations. For this purpose, the cross-section of the parallel and pre-parallel

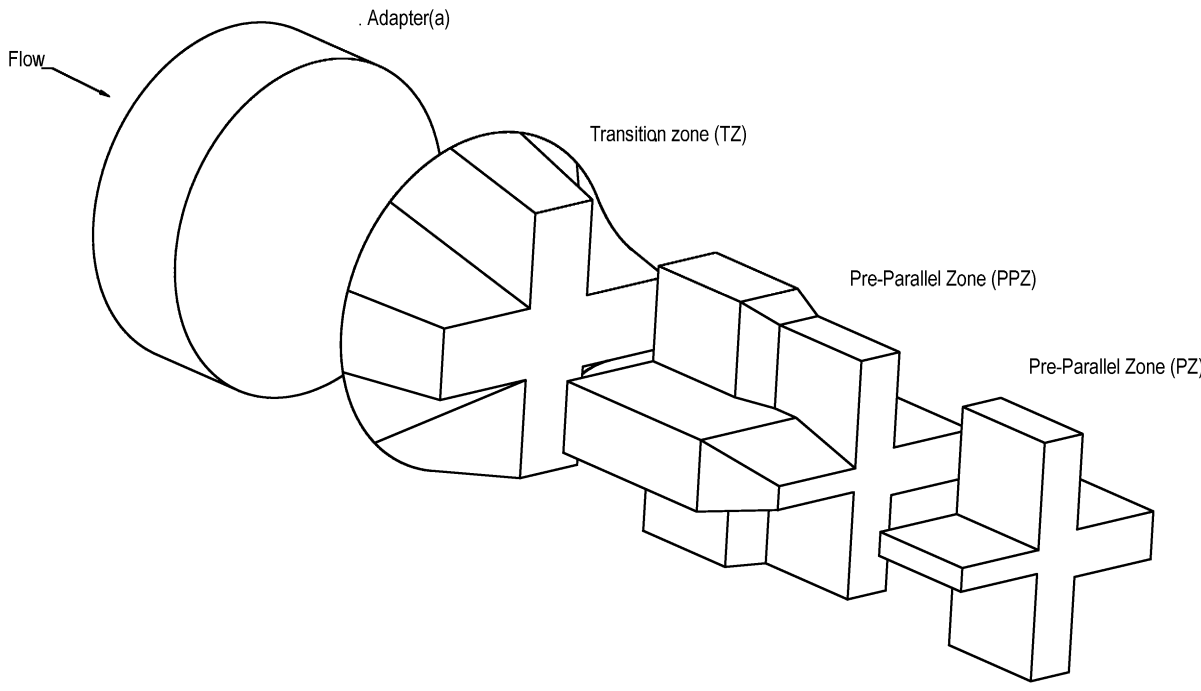

Fig. 1. Flow channel of a profile extrusion die split in the main geometrical zones.

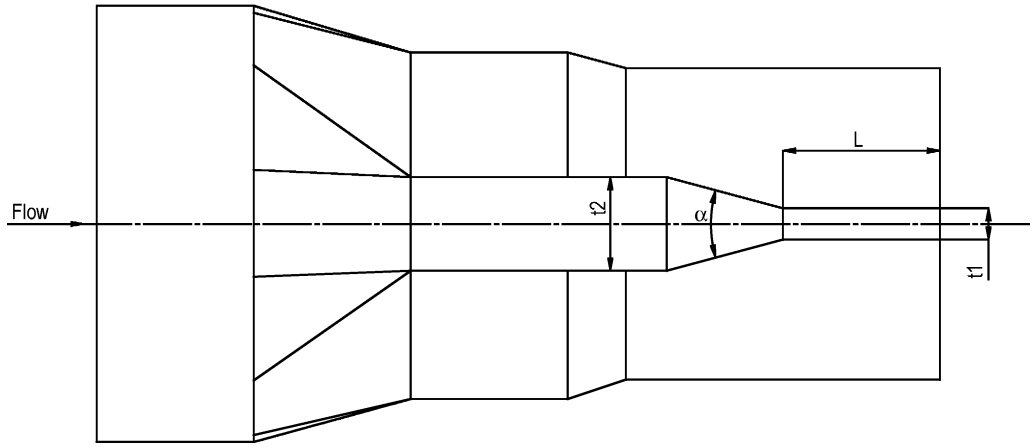

Fig. 2. Side view of the flow channel illustrated in Fig. 1 showing the geometrical controllable parameters considered in the definition of the pre-parallel zone.

zones is divided into elemental sections (ESs) (see Fig. 5(a) for an example). Then, assuming that the flow is balanced, the cross-section of the parallel zone is iteratively defined anticipating for the effects of post-extrusion phenomena and based on the maximum flow rate imposed by the maximum shear stress of the polymer melt (τ_{crit}) and/or by the maximum admissible pressure drop. The initial trial length of each elemental section of the parallel zone is then computed in order to approach the assumed flow balanced condition. Finally, the initial geometry of the flow channel is created using a pre-defined compression ratio (or entrance thickness, t_2) and a convergence angle dictated by the maximum admissible normal stress of the melt (σ_{crit}). As a first attempt the constructive solution adopted should be the conventional one, i.e., flow channel without separating walls to avoid the formation of weld lines.

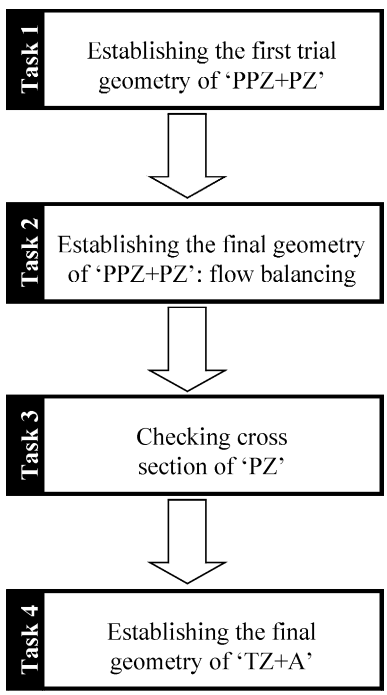

Fig. 3. Main steps involved in the design of an extrusion die.

Task 2 consists of the iterative definition of the geometry of the pre-parallel zone required to balance the flow, using numerical modelling of the flow on the pre-parallel and parallel zones. If the final balanced geometry results in parallel zones that are too short to allow the relaxation of the stresses developed in upstream convergent zones, another constructive solution must be sought with the allocation of separating walls between the most critical elemental sections. These flow separators start at the entrance of PPZ and end some millimetres before the die exit [13]. This second constructive solution enables the independent control of each elemental section [9,10], but it shall be avoided whenever possible as it induces the formation of weak weld lines close to the die exit, affecting the mechanical performance of the extruded profile.

After reaching the required flow balance, the cross-section of the parallel zone previously established is checked (Task 3) by performing a numerical simulation of the flow in the pre-parallel and parallel zones and free surface.

Finally, in Task 4, the transition zone and adapter are generated and a final global check is carried out.

The global methodology presented in Fig. 3, is shown in more detail in Fig. 4. It includes the input data, the sequence of calculations, the conditions to check and actions to take whenever the limiting conditions are exceeded.

The main steps of the flowchart in Fig. 4 (numbered from 1 to 16) are described as follows:

Task 1 — *Establishing the first trial geometry of* '*PPZ* + *PZ*'.

Step 1. The cross-section of the parallel zone is considered equal to that of the profile to be extruded and is divided in elemental sections (ESs).

Steps 2/3. The initial flow rate to be used in the calculations is defined in several steps. The maximum

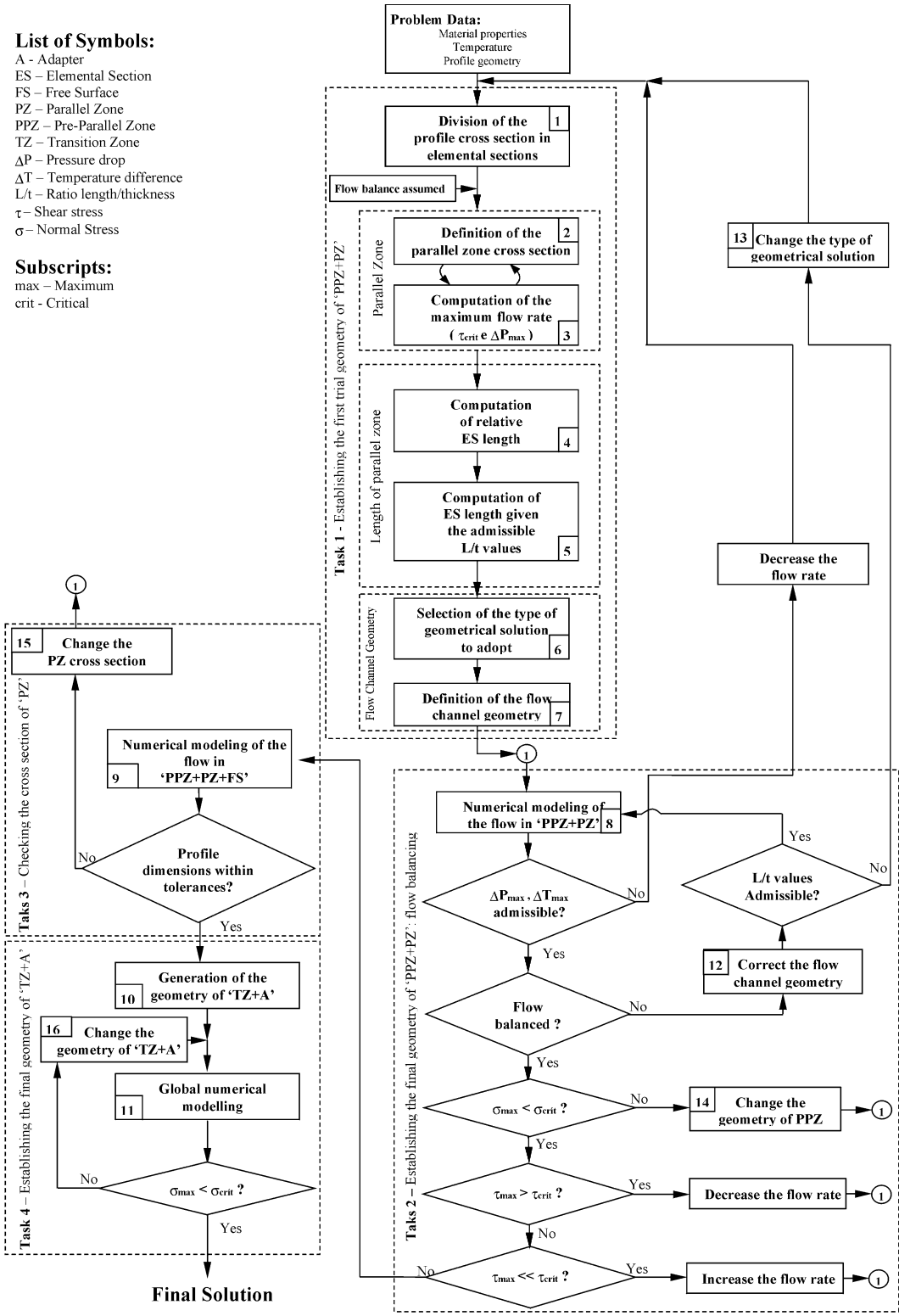

Fig. 4. Detailed flow chart of the design process depicted in Fig. 3.

flow rate in each ES is determined by the critical shear stress of the melt, via an analytical approach [14], considering a one-dimensional isothermal flow in the slit. Assuming flow balance, the relative flow rate in each ES is determined allowing the identification of the critical one, its maximum flow rate and, therefore, the corresponding flow rates in the remaining ES. The dimensions of the cross-section of each ES of the parallel zone defined in Step 1 are now analytically modified using the corresponding local flow rates and

analytical relations to anticipate the effects of the post-extrusion phenomena [14]. These calculations are necessarily iterative due to the interdependence between extrudate cross-section and flow rate.

Step 4. Analytical calculation of the relative length of each ES of the parallel zone in order to ensure the same pressure drop for all the paths at the corresponding prescribed local flow rates, considering a one-dimensional flow of a power-law fluid in a slit.

Step 5. Determination of the absolute length of each parallel zone, considering the limiting value of the ratio between length (L) and thickness (t) [13]. This ratio is generally high (between 7 and 15), allowing for consideration of a die-swell essentially dependent on the shear flow occurring at the PZ and, therefore, less sensitive to variations in operating conditions and almost independent of the extensional flow occurring upstream at the PPZ. This limiting value of L/t is, therefore, dependent on the maximum relaxation time of the melt and the residence time in the PZ.

Step 6. Definition of the first trial of the selected constructive solution to be adopted. It must provide the possibility of changing independently the length and dimensions of the elemental sections of the parallel and pre-parallel zones. The initial constructive solution should be the conventional one, i.e., without separating walls.

Step 7. Definition of the first trial geometry of the die exit zone, i.e., pre-parallel zone (PPZ) and parallel zone (PZ). To avoid the occurrence of melt fracture, the maximum convergence angle of each section of the PPZ is determined analytically using the criteria of the critical normal stress of the melt [14,15].

Task 2 — *Establishing the final geometry of* '*PPZ* + *PZ*': *flow balancing*.

Step 8. Generation of the computational grids for the flow domain 'PPZ + PZ' and corresponding numerical simulation of the flow to determine the local flow fields. From the local flow fields the zone bulk velocities can be determined. Ideally, the numerical simulations must be carried out considering a three-dimensional non-isothermal flow of viscoelastic fluids.

Step 12. If necessary, new adjustments of the length of PZ and/or dimensions of PPZ should be carried out to balance the flow.

Step 13. If the ratio L/t of any elemental PZ becomes lower than a minimum limiting value, the solution of the problem is restarted, considering another type of constructive solution such as the allocation of flow separators between some or all the ES.

Step 14. If the critical normal stress of the melt, σ_{crit}, is exceeded, the convergence of the PPZ must be reduced.

Task 3 — *Checking the cross-section of PZ.*

Step 9. After checking/correcting for admissible conditions on pressure drop, temperature increase, shear stress and normal stress, flow balancing requirement and impossibility of increasing the flow rate, a numerical simulation of the flow in the domain 'PPZ + PZ + FS (free surface)' must be performed in order to check the final dimensions of the extrudate. The FS zone should only be included at this stage in order to increase the efficiency of the process, reducing the total time required to perform the simulations.

Step 15. If the dimensions of the extrudate are outside specifications, the cross-section of the parallel zone must be changed.

Task 4 — *Establishing the geometry of* '*TZ* + *A*'.

Step 10. If the extrudate dimensions are within the tolerances previously defined, the next step will consist on the automatic definition of the geometry of the transition zone (TZ) and adapter (A).

Step 11. At this stage a global numerical simulation must be performed in the global flow domain 'A + T + PPZ + PZ + FS'. The adapter and transition zone are only considered at this stage because they are not expected to significantly influence the die performance.

Step 16. If the critical normal stress of the melt, σ_{crit}, is exceeded, the convergence of the adapter must be reduced.

This methodology is currently being implemented and in this work only the initialisation and flow balancing procedures (Tasks 1 and 2) are tested. Considering this objective, in the case studies used for this purpose the fluid is modelled considering an isothermal generalised Newtonian constitutive equation, an option that does not affect the generality of the test performed.

3. Outline of the numerical procedure for calculating the flow field

As described in the previous section, the flow field needs to be calculated in steps 8, 9 and 11 of the methodology. This is accomplished by a self-contained part of the code that has been developed for the computation of viscoelastic flows and is described and tested in detail in a series of papers [12,17,18], which the reader should consult for detailed information. Here, we just give a quick overview of the calculation procedure, which solves a set of equations for fluid flow.

The basic equations to be solved are those expressing conservation of mass

$$\frac{\partial u_j}{\partial x_j} = 0 \tag{1}$$

of linear momentum

$$\frac{\partial \rho u_i}{\partial t} + \frac{\partial \rho u_j u_i}{\partial x_j} = -\frac{\partial p}{\partial x_i} + \frac{\partial \tau_{ij}}{\partial x_j} \tag{2}$$

and a constitutive rheological equation for the stress field τ_{ij}. In these equations, u_i is the velocity component for the Cartesian axis, ρ the fluid density and p an isotropic pressure. In the present computations the generalised Newtonian rheological constitutive equation was considered

$$\tau_{ij} = \eta(\dot{\gamma})\left(\frac{\partial u_i}{\partial x_j} + \frac{\partial u_j}{\partial x_i}\right) - \frac{2}{3}\eta(\dot{\gamma})\frac{\partial u_k}{\partial x_k}\delta_{ij} \tag{3}$$

where η is the dynamic viscosity of the fluid. The velocity divergence in the last term vanishes for incompressible flows, but is kept in the code for stability reasons. The dynamic viscosity is a function of the second invariant of the rate of deformation tensor $\dot{\gamma} \equiv \sqrt{2\,\mathrm{tr}\,D^2}$ where

$$D_{ij} = \frac{1}{2}\left(\frac{\partial u_i}{\partial x_j} + \frac{\partial u_j}{\partial x_i}\right) \tag{4}$$

and η in the specific tests of this paper is given by the Bird–Carreau equation [19]

$$\eta(\dot{\gamma}) = \eta_\infty + \frac{\eta_0 - \eta_\infty}{(1 + (\lambda\dot{\gamma})^2)^{(1-n)/2}} \tag{5}$$

where η_∞ and η_0 are the limit viscosities for high and low shear rates, respectively, λ a time constant and n the flow index.

In this first work, isothermal conditions are assumed and, therefore, there was no need to solve the energy equation. In the future these assumptions will be relaxed to allow for viscoelastic melt flow in the die and non-isothermal conditions with the inclusion of the energy conservation equation with provision for viscous dissipation.

These equations were transformed into a general, non-orthogonal coordinate system for calculating the pressure, the Cartesian velocity components and the Cartesian stress tensor components. The resulting differential transport and constitutive equations were then discretised following the finite-volume approach of Patankar [20], but adapted for collocated, non-orthogonal grids, as described in Oliveira [16]. To this aim, and prior to discretisation, the equations are integrated over control volumes (CVs) forming the computational mesh and are thus transformed into algebraic equations which relate values of velocity, stress and pressure at a given CV to values at surrounding CVs. The resulting algebraic equations for velocity and stress have the form

$$a_P^\phi \phi_{i,P} = \sum_{\mathrm{nb}} a_{\mathrm{nb}}^\phi \phi_{i,\mathrm{nb}} + Su^\phi \tag{6}$$

where $\phi_{i,P}$ represents a velocity or stress component at the central node of the control volume P, as a function of the neighbour values $\phi_{i,\mathrm{nb}}$. The coefficients of the algebraic equations are a_P^ϕ and a_{nb}^ϕ, which depend on the particular variable of the equation (velocity or stress components) and of the computational molecule, i.e., the interpolation and discretisation schemes used to calculate face values and derivatives of ϕ, respectively. The independent term is represented by Su^ϕ.

The description of the computational rheology code is rather long. It is a self-contained programme which has been described and tested elsewhere [12,17,18] and therefore the reader interested in further details should consult those references. Here, it suffices to say that the discretisation and interpolation schemes are based on the second-order central differencing scheme and the deferred correction approach was used for the convective terms in the momentum equations, in order to ensure numerical stability. Note that, since the constitutive equation (Eq. (3)) is explicit on the stress, its components are immediately calculated from previous iteration values of the velocity field. The solution algorithm was a modified version of the SIMPLEC algorithm of van Doormal and Raithby [21] adapted for time marching as explained in Issa and Oliveira [22], where details can be found of the particular procedure used to evaluate mass fluxes at cell faces. The linearised algebraic equations for the three Cartesian velocity components are first solved sequentially, with a bi-conjugate gradient method, and where the pressure-gradient term is based on pressure values from the previous time-step. These pressures are then corrected in such a way that forces the velocity field to satisfy the continuity equation. The overall algorithm is thus based on successive applications of momentum predictors, followed by pressure/velocity correctors, until a steady-state solution is achieved. To monitor convergence to a steady solution, the norms of the residuals of all the discretised equations are required to fall below a relative tolerance of 10^{-4}.

Three-dimensional grids were required for these simulations which were sufficiently fine to capture the main flow characteristics and to show the feasibility of the methodology. Typically, for an elemental zone having a thickness of 1 mm, width of 5 mm and length of 10 mm, a grid of $6 \times 30 \times 60$ uniform CVs was used. Fig. 5(c) shows a typical mesh used in the calculations with the geometry depicted in Fig. 5(a) and (b).

4. Case studies

The polymer used in the simulations was a polypropylene homopolymer extrusion grade, Novolen PPH 2150, from Targor. Its rheological behaviour was experimentally characterised by capillary and rotational reometries, at 230°C, and its shear viscosity was least-squared fitted by a Bird–Carreau constitutive equation (Eq. (5)) that produced the following parameters: $\eta_\infty\,(\mathrm{Pa\,s}) = 0$, $\eta_0\,(\mathrm{Pa\,s}) = 5.58 \times 10^4$, $\lambda\,(\mathrm{s}) = 3.21$ and $n = 0.3014$.

The performance of the methodology proposed for flow balancing (Task 2) was assessed by testing the design of two similar extrusion dies for the production of cross shaped

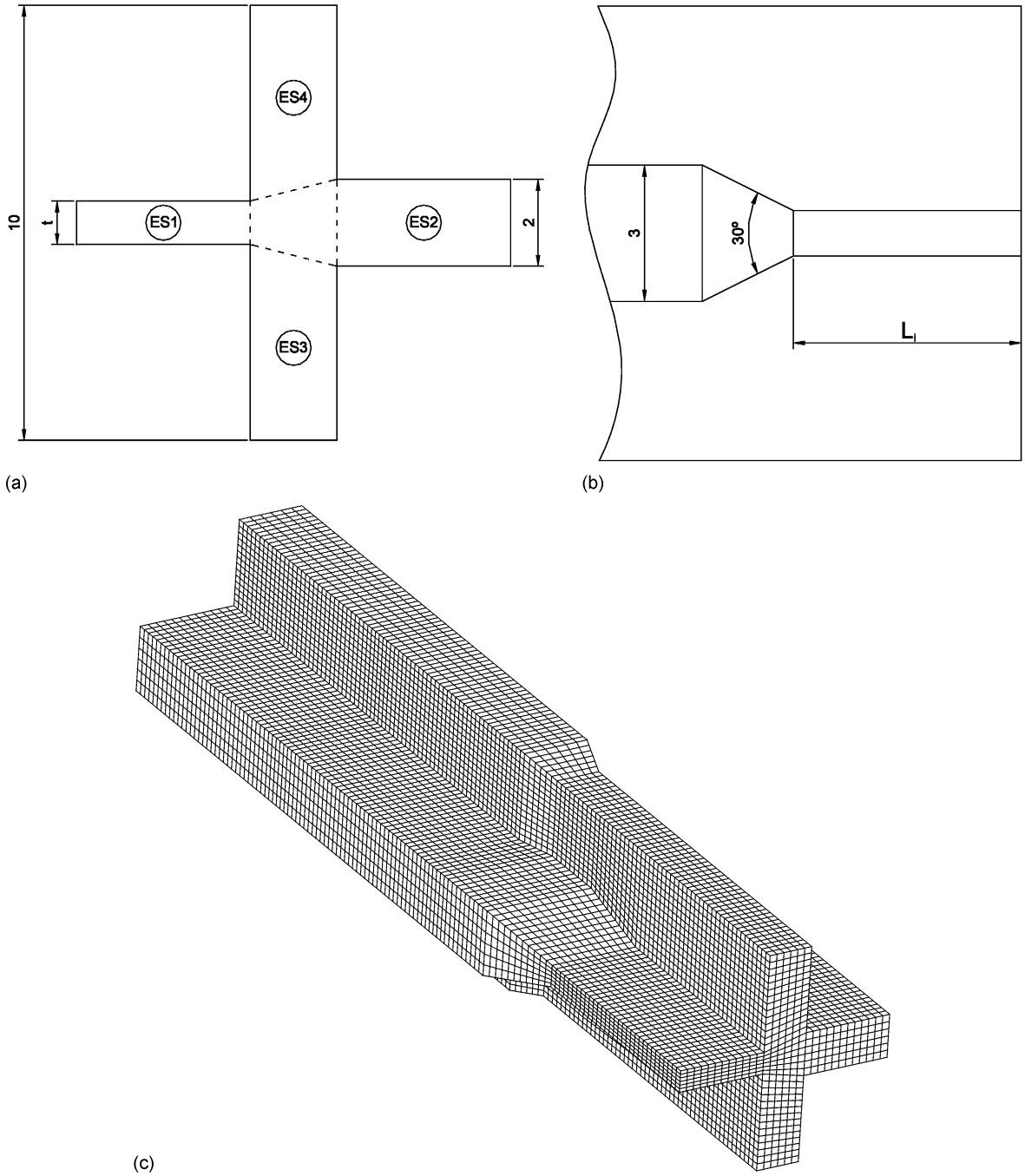

Fig. 5. Flow channel of the profile die used as a case study (dimensions in mm): (a) cross-section of the parallel zone (PZ) and elemental sections (ESs) considered; (b) side view; (c) typical mesh used in the calculations.

profiles, called Cross-B die and Cross-U die. The profiles have the parallel zone cross-section depicted in Fig. 5(a) with three legs having a thickness of 2.0 mm and a thinner fourth leg of thickness t. The different thicknesses of the legs result in an unbalanced flow because the thinner leg is more flow restrictive. The difference between the two dies concerns the thickness of the thinner leg (t in Fig. 5(a)), which has the value of 1.8 mm for Cross-B die and 1 mm for Cross-U die. From a flow-balance point of view, the former is expected to be almost balanced (Cross-B), and the latter strongly unbalanced (Cross-U).

A flow rate was imposed corresponding to an average velocity of 100 mm/s at the die exit and the flow was considered isothermal. Considering the objective of these case studies, the simulations of the flow were only performed in the die zones relevant for this purpose, i.e., PPZ and PZ, as determined by the proposed methodology. The geometry of the die was considered similar to the one shown

in Figs. 1 and 2. In a previous work [23], it was concluded that the parameter that most influences the flow balance is the length with constant thickness (L). As a consequence, the other dimensions of the PPZ, defined in Fig. 5(b), were fixed (entrance thickness: 3 mm for all legs; convergence angle (α): 30°), i.e., only the lengths L_i of each ES needed to be determined. In each iteration the correction of each ES length was based on the ratio between the computed and required average velocities: when the calculated velocity was higher than the required, the ES length was increased in order to augment the flow restriction, and vice versa. The maximum and minimum admissible values for ratio L/t were considered to be 15 and 1, respectively. As stated before (Step 5 of the methodology), L/t values below 7 are not advisable. However, it would not be prudent to reject a trial geometry perfectly balanced having a L/t slightly lower, since the limit values are merely dictated by industrial practice. Therefore, in this work the quality of each geometry is assessed by a function (objective function, F_{obj}), which combines the two individual criteria (flow balancing and ratio L/t) affected by different weights:

$$F_{obj} = \sum_{i=1}^{4} \left\{ \alpha \left(1 - \frac{V_i}{V_{av}} \right)^2 + k(1-\alpha) \left[1 - \frac{(L/t)_i}{(L/t)_{opt}} \right]^2 \right\} \quad (7)$$

with $k = 0$ for $(L/t)_i \geq (L/t)_{opt}$ and $k = 1$ for $(L/t)_i < (L/t)_{opt}$, where V_{av} and V_i are the average velocities of the extrudate and of the flow in each ES, respectively, $(L/t)_i$ the ratio between length and thickness of each ES, $(L/t)_{opt}$ the optimum value for the ratio L/t (considered to be 7), and α the relative weight (considering the higher relative importance of the flow balance criterion, α was considered to be 0.75).

The value of the objective function decreases with increasing performance of the die, being zero for a balanced die having all the ES lengths in the admissible range.

A routine was also developed for the automatic definition of the geometry, which then served as input to the existing pre-processor of the computational rheology code that generated the computational grid required for the numerical flow simulations. The developed routine, the pre-processor and the CR code were integrated smoothly as part of the whole die design code.

5. Results and discussion

Initially, the parallel zone cross-section was divided in four elemental sections, ES1–ES4, as shown in Fig. 5(a). Note that the region defined by the intersection of the four legs was not considered as an independent zone due to the impossibility of controlling independently its geometry. However, this zone will also become balanced when the average flow velocity in all the elemental sections, ES1–4, is equal to the extrusion average linear velocity. Given the symmetry of the cross-section, the flow through ES3 and ES4 is similar and the corresponding results are presented together.

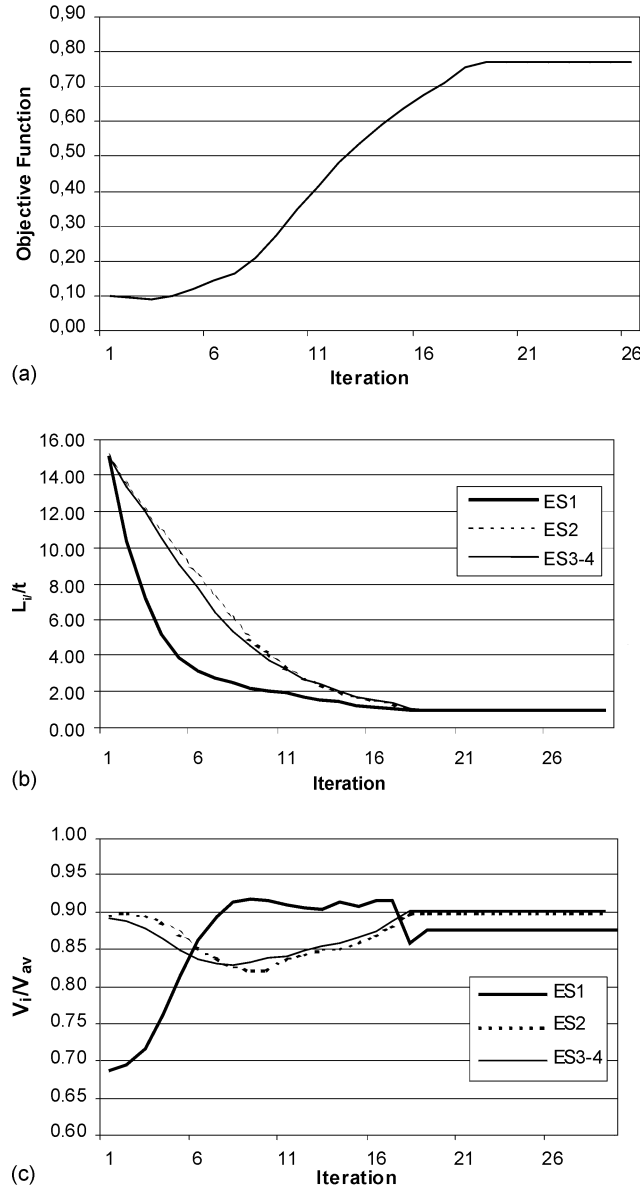

Fig. 6. Results of simulations performed in successive iterations for Cross-B die: (a) objective function; (b) ratio length/thickness of the parallel zone of each elemental section; (c) relative average velocity in each elemental section.

The results obtained for the Cross-B die are illustrated in terms of objective function in Fig. 6(a), ratio L/t in Fig. 6(b) and relative average velocity in Fig. 6(c). As indicated by the objective function, the best solution is obtained around iteration 4 with a value of just under 0.1. However, it must be noted that even in this case the best solution for the flow balance is a geometry having very small L/t ratios (iteration 20 in Fig. 6(b) and (c)), which corresponds to a high value of the objective function (see Fig. 6(a)). That is a consequence

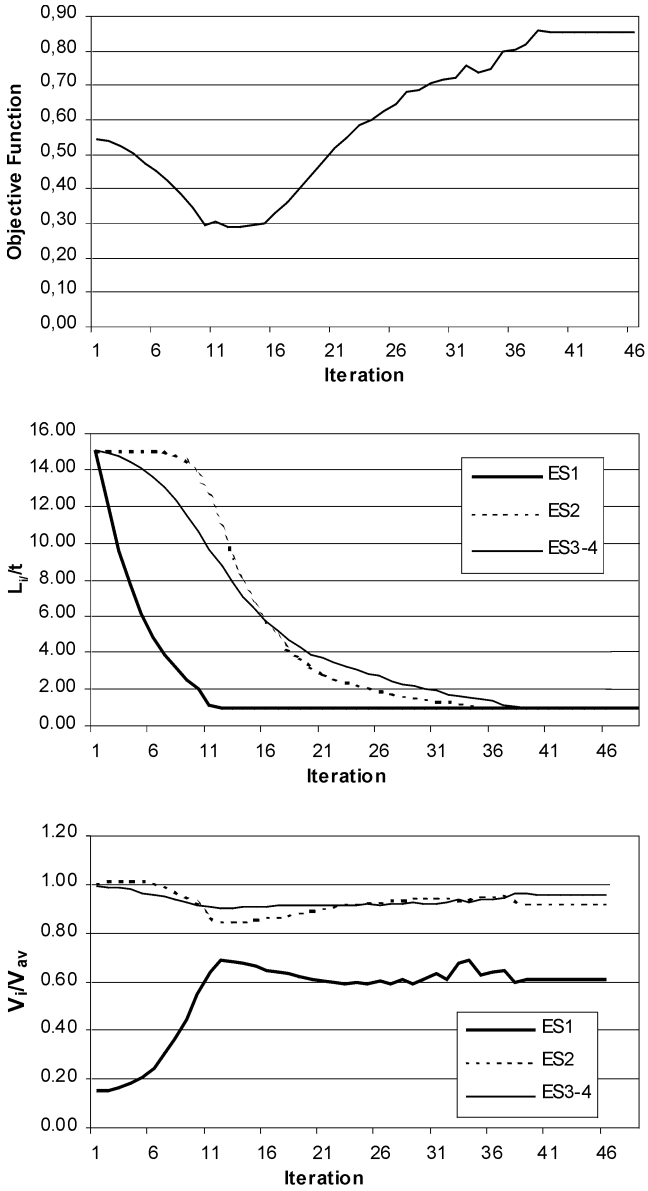

Fig. 7. Results of simulations performed in successive iterations for Cross-U die: (a) objective function; (b) ratio length/thickness of the parallel zone of each elemental section; (c) relative average velocity in each elemental section.

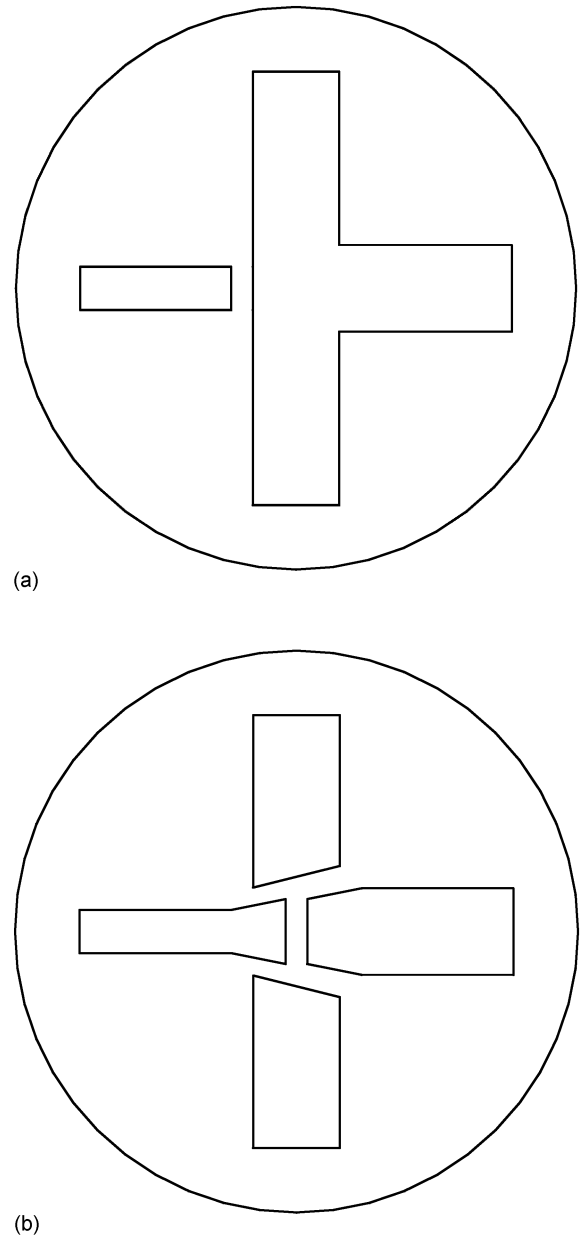

Fig. 8. Cross-section of the parallel zone before the junction of the independent streams: (a) Cross-U1 solution, using one flow separator; (b) Cross-U2 solution, using three flow separators.

of the small restriction imposed by the intersection zone, which induces the progressive reduction of the length of all neighbouring ES in order to avoid fluid coming into that zone.

For the Cross-U die the results of the simulation are presented in Fig. 7 in a similar way to that of Fig. 6. It can be concluded that for the Cross-U die the algorithm was unable to reach a realistic geometrical solution, as shown by the relatively high (0.3) minimum value of the objective function. In fact, the thinner section (ES1) remains too restrictive even when an unacceptable low value of L/t is considered. As a consequence, another constructive solution, involving the allocation of flow separators, was tried and the two possibilities shown in Fig. 8 were considered: Cross-U1 solution uses one separator to isolate the critical sub-section (ES1), whereas in Cross-U2 three separators are used to isolate all the ES and to eliminate the intersection region.

The results obtained with the Cross-U1 geometry are plotted in Fig. 9 and show that around iteration 5 the flow is almost balanced using L/t values within the admissible range, corresponding to a value of around 0.05 for the objective function. However, due to the existence of an intersection zone there is a progressive reduction of the

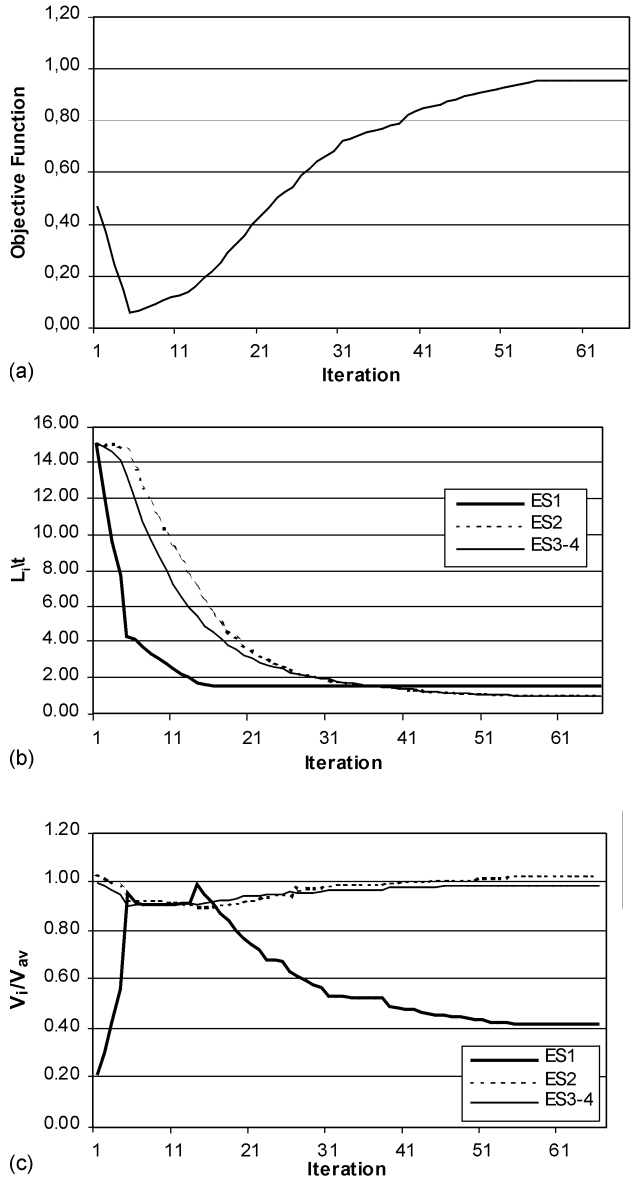

Fig. 9. Results of simulations performed in successive iterations for Cross-U1 solution: (a) objective function; (b) ratio length/thickness of the parallel zone of each elemental section; (c) relative average velocity in each elemental section.

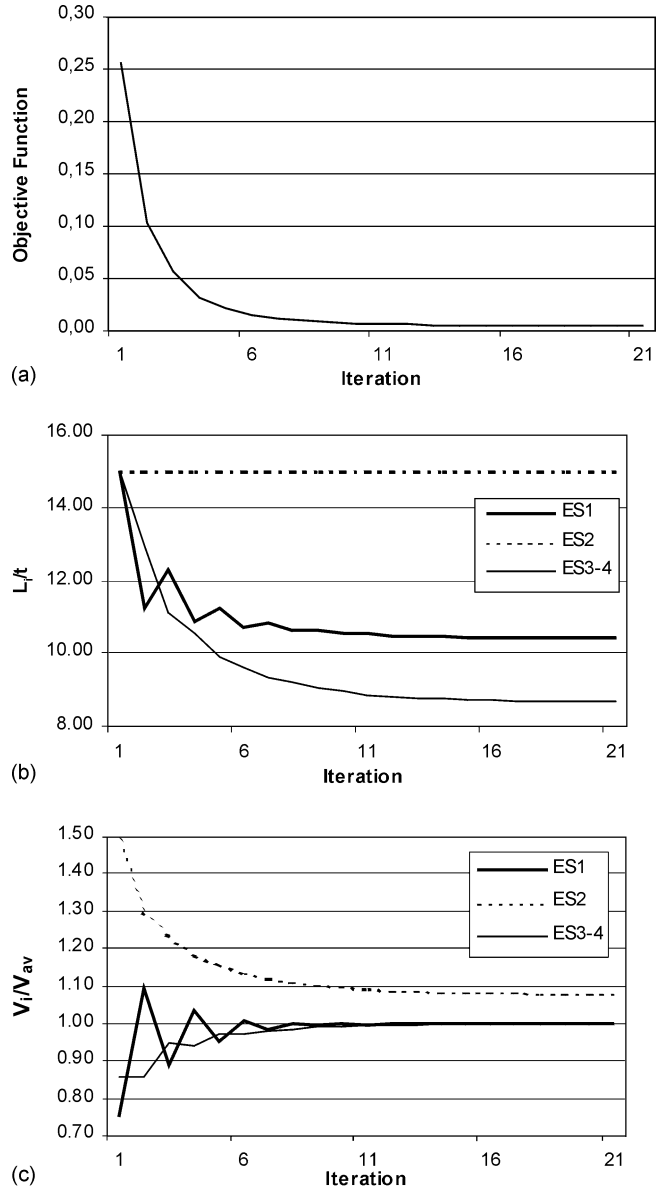

Fig. 10. Results of simulations performed in successive iterations for Cross-U2 solution: (a) objective function; (b) ratio length/thickness of the parallel zone of each elemental section; (c) relative average velocity in each elemental section.

length of all ES in the subsequent iterations, as happened before with geometry Cross-B, leading to the increase of the objective function. With the Cross-U2 geometry this problem was solved with the suppression of the intersection zone along the paths defined by the separators. In this particular case it was possible to generate successive better geometries and to reach a well balanced final solution, within the pre-defined *L*/*t* limits, with the lowest value of the objective function (around 0.01), as shown in Fig. 10.

Contours of the axial velocity are shown in Fig. 11 for three cases: the initial iteration used with Cross-U die and the best results obtained for Cross-U1 and Cross-U2 solutions. The progression from a strongly unbalanced situation (Cross-U) to an almost balanced case (Cross-U2) is well shown.

It should be noted that the Cross-U2 alternative, despite being the most balanced case, does not guarantee the best solution from the mechanical point of view, as it promotes the formation of several weld lines. The lateral flow that takes place after the junction of the independent streams, just before the die exit, will contribute to enhance the strength of the weld lines, but it may be insufficient to guarantee the adequate mechanical performance of the extrudate.

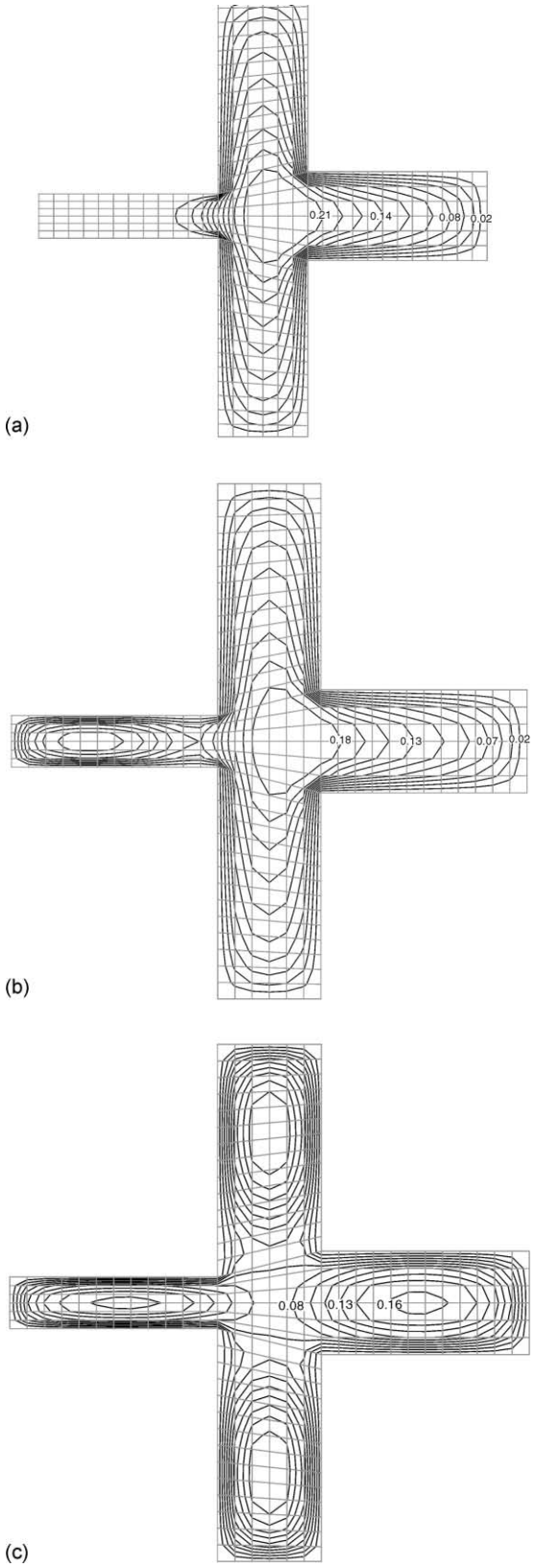

Fig. 11. Contours of the axial velocity (m/s) computed for: (a) initial trial geometry (iteration 1) of Cross-U die; (b) best result (iteration 5) obtained for Cross-U1 solution; (c) final geometry (iteration 21) of Cross-U2 solution.

6. Conclusions

In this work the main steps needed for the automatic design of extrusion dies for profiles have been identified and a general methodology to perform this task is presented. The methodology does not yet include an optimisation algorithm, but already uses a 3D computational code for performing numerical simulations of the flow. This code is capable of viscoelastic computations although the predictions here were based on inelastic shear-thinning fluids. In this paper only the part of the methodology related to flow balancing was tested successfully. To assess the quality of the calculated geometries an objective function that takes into account the flow balancing and the ratio L/t of the parallel zone was used and the main results were the following:

1. The insertion of a pre-parallel zone proved to allow the systematic search of a flow balanced geometry.
2. Accentuated differences in thickness among the channels of a cross-shaped die lead to very short parallel zones, therefore requiring the allocation of flow separators between the more restrictive sections. This practice may be needed even for apparently balanced geometries that have low flow restriction (intersection) zones.
3. The insertion of flow separators was shown to be a good solution in terms of flow balancing, but it must be well pondered in order to minimise the risk of mechanical failure of the extrudate.
4. The objective function proposed has shown to be an adequate method for quantitative evaluation of the performance of the extrusion dies used in this work.

References

[1] Polyflow, Fluent Inc.
[2] Diecalc, Rapra Technology Ltd.
[3] G. Menges, M. Kalwa, J. Schmidt, FEM simulation of heat transfer in polymer processing, Kunstst. 77 (1987) 797.
[4] J. Vlachopoulos, P. Behncke, J. Vlcek, POLYCAD: a finite element package for polymer process analysis and design, Adv. Polym. Tech. 9 (1989) 147.
[5] D.H. Sebastian, R. Rakos, Interactive software package for the design and analysis of extrusion profile dies, Adv. Polym. Tech. 5 (1985) 333.
[6] H.-P. Wang, Designing profile dies CAD removes the guess, Plastics Technol. (February) (1996) 46.
[7] V. Legat, J.M. Marchal, Die design: an implicit formulation for the inverse problem, Int. J. Num. Methods Fluids 16 (1993) 29.
[8] M.P. Reddy, E.G. Schaub, L.G. Reifschneider, H.L. Thomas, Design and optimization of three-dimensional extrusion dies using adaptive finite element method, ANTEC '99, 1999.
[9] P. Hurez, P.A. Tanguy, D. Blouin, A new design procedure for profile extrusion dies, Polym. Eng. Sci. 36 (1996) 626.
[10] J. Svabik, L. Placek, P. Saha, Profile die design based on flow balancing, Intern. Polym. Process. XIV (1999) 247.

[11] I. Szarvasy, J. Sienz, J.F.T. Pitman, E. Hinton, Computer aided optimisation of profile extrusion dies, Intern. Polym. Process. XV (2000) 28.
[12] P.J. Oliveira, F.T. Pinho, G.A. Pinto, Numerical simulation of non-linear elastic flows with a general collocated finite-volume method, J. Non-Newt. Fluid Mech. 79 (1998) 1.
[13] W. Michaeli, Extrusion Dies for Plastic and Rubber, Hanser, Munich, 1992.
[14] O.S. Carneiro, J.A. Covas, Design and assessment of mandrel pipe dies, Plast. Rubb. Comp. Proc. Appl. 24 (1995) 79.
[15] F.N. Cogswell, Converging flow of polymer melts in extrusion dies, Polym. Eng. Sci. 12 (1972) 64.
[16] P.J. Oliveira, Computer modelling of multidimensional multiphase flow and application to T-junctions, Ph.D. Thesis, Imperial College of Science, Technology and Medicine, 1992.
[17] P.J. Oliveira, F.T. Pinho, Numerical procedure for the computation of fluid flow with arbitrary stress–strain relationships, Num. Heat Transfer B 35 (1999) 295.
[18] P.J. Oliveira, F.T. Pinho, Plane contraction flows of upper convected Maxwell and Phan–Thien–Tanner fluids as predicted by a finite volume method, J. Non-Newt. Fluid Mech. 88 (1999) 63.
[19] D.G. Baird, D.I. Collias, Polymer Processing — Principles and Design, Butterworth–Heinemann, London, 1995, pp. 11 (Chapter 2).
[20] S.V. Patankar, Numerical Heat Transfer and Fluid Flow, Hemisphere, Bristol, 1982.
[21] J.P. van Doormal, G.D. Raithby, Enhancements of the SIMPLE method for predicting incompressible fluid flows, Num. Heat Transfer 7 (1984) 147.
[22] R.I. Issa, P.J. Oliveira, Numerical predictions of phase separation in two phase flow through T-junctions, Comput. Fluids 23 (1994) 347.
[23] J.M. Nóbrega, O.S. Carneiro, F.T. Pinho, P.J. Oliveira, Flow balancing in extrusion dies for profiles, in: Proceedings of the Second National Meeting of the Portuguese Society of Rheology, 2000 (in Portuguese).